Available online at www.sciencedirect.com
SCIENCE DIRECT®
Journal of Hydrology xx (2003) 1–18
Journal of Hydrology
www.elsevier.com/locate/jhydrol

Interseasonal covariability of Sierra Nevada streamflow and San Francisco Bay salinity

Michael D. Dettinger*, Daniel R. Cayan

US Geological Survey, Scripps Institution of Oceanography, University of California San Diego, 9500 Gilman Drive, Dept. 0224, La Jolla, CA 92093-0224, USA

Received 7 February 2002; accepted 20 February 2003

Abstract

The ecosystems of the San Francisco Bay estuary are influenced by the salinity of its waters, which in turn depends on flushing by freshwater inflows from the western slopes of the Sierra Nevada. Estimates of full-natural flows in eight major rivers that flush the Bay are analyzed here by extended empirical-orthogonal-function analyses to characterize distinct 'modes' of seasonal flow and runoff variability. These modes provide a clear identification of the seasons in which the various rivers respond to hydroclimatic forcings and the seasons during which the rivers most strongly affect San Francisco Bay salinities. About 60 percent of the runoff variability is shared by the rivers over the course of a year but season-to-season differences among the rivers are more subtly distributed. Autumn and winter streamflows respond directly to concurrent (autumn and winter) precipitation and temperatures. Autumn and winter salinities are dominated by these flows, which in each season reflect mostly variations in flows from the central Sierra Nevada and the large Sacramento River. In contrast, spring runoff-rate and streamflow modes are functions of precipitation and temperature during the entire wet (winter and spring) season and are dominated by rivers of the central and southern Sierra Nevada. In turn, the critical spring salinities depend most on the streamflow fluctuations in those central and southern rivers.

Keywords: Surface water flow; Estuarine salinity; Climate; California; Sierra Nevada; San Francisco Bay

1. Introduction

San Francisco Bay is the third largest estuary in the United States and is outlet for runoff from the Sierra Nevada, California's major watershed. The health of San Francisco Bay ecosystems is tied to the salinity of its waters (e.g. Jassby et al., 1996; Kimmerer and Orsi, 1996). The salinity of the Bay, in turn, depends on freshwater inflows from the Sacramento–San Joaquin Delta, the salinity of the coastal ocean, vertical and lateral mixing of the Bay by tides and winds, and sea-level height (Peterson et al., 1995, 1996). In response to the Mediterranean climate and runoff regime of California, salinities are least during winter and spring and increase during summer and autumn of most years, with winter-to-summer salinity differences averaging about 7 parts per thousand at the outlet of the Bay. Salinities vary markedly within the Bay from year to year, from nearly undiluted sea water in some years to nearly fresh in others.

* Corresponding author.
E-mail address: mddettin@usgs.gov (M.D. Dettinger).

0022-1694/03/$ - see front matter © 2003 Published by Elsevier Science B.V.
doi:10.1016/S0022-1694(03)00078-7

In response to the competing needs of San Francisco Bay ecosystems, upstream endangered species, and upstream water uses, targets for salinities in the Bay during the February–June 'season' have been part of the management of the Bay since 1995 (Jassby et al., 1995; Peterson, 1995; Kennish, 2000). The primary example of these salinity standards is the 'X2' standard, which mandates that surface salinities at selected sites in the northern estuary not rise above 2 parts per thousand for more than a limited number of days during the February–June season (California Department of Water Resources, 2000), with the targeted number of days conditioned each year by antecedent freshwater flow rates in the Sierra Nevada. Such targets will be met mostly through management of freshwater inflows to the Bay, which are supplied mostly by eight major rivers that drain the western Sierra Nevada through the Sacramento and San Joaquin Valleys (from south to north, and—generally—highest altitude to lowest): the San Joaquin, Merced, Tuolumne, Stanislaus, American, Yuba, Feather, and Sacramento Rivers (Fig. 1). The seasonal variations of their streamflow rates are complexly intertwined and, together, dominate the long-term

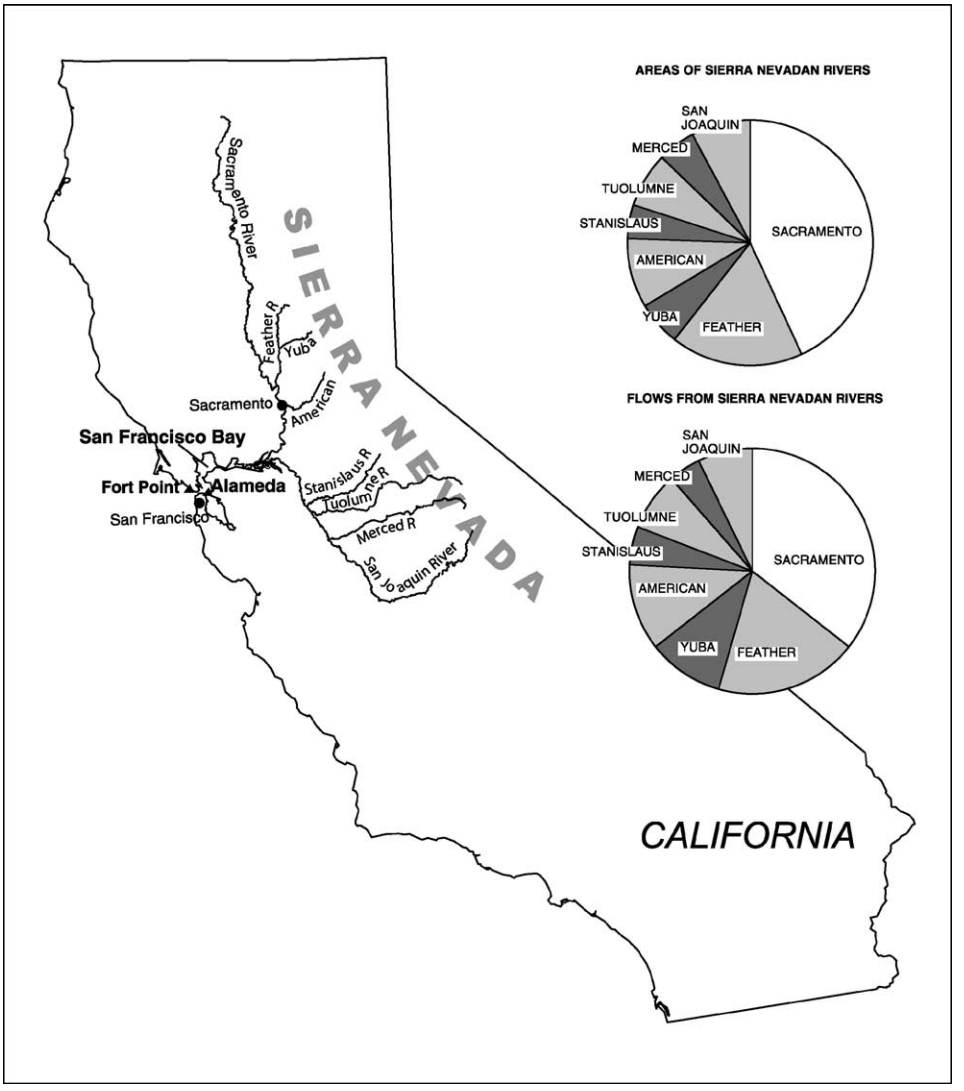

Fig. 1. Locations of Sierra Nevada, eight major rivers, and features around San Francisco Bay.

Table 1
Correlations between Fort Point salinities and Sacramento/San Joaquin River flows, 1922–89. Bold values—significantly different from zero at 99-percent level

Salinity	Sacramento River flows				San Joaquin River flows			
	Autumn	Winter	Spring	Summer	Autumn	Winter	Spring	Summer
Autumn	**−0.60**	−0.26	**−0.32**	**−0.43**	**−0.65**	−0.20	−0.19	−0.26
Winter	**−0.53**	**−0.79**	**−0.65**	**−0.53**	**−0.52**	**−0.78**	**−0.77**	**−0.72**
Spring	−0.24	**−0.46**	**−0.76**	−0.26	−0.19	**−0.44**	**−0.74**	**−0.60**
Summer	**−0.35**	**−0.43**	**−0.70**	**−0.33**	**−0.36**	**−0.47**	**−0.60**	**−0.66**
Next Autumn	**−0.34**	**−0.46**	**−0.53**	**−0.36**	**−0.42**	**−0.45**	**−0.60**	**−0.57**

(months to years) variability of San Francisco Bay salinities. Management of those rivers for salinity control in San Francisco Bay requires improvements in understanding of their seasonal covariability.

1.1. Problem

Some of the streamflow covariability, and its role in confusing the sources of salinity variations in San Francisco Bay, can be seen in correlations between seasonal streamflows in the northernmost and southernmost of the eight rivers (the Sacramento and San Joaquin Rivers, respectively) and San Francisco Bay salinities (Table 1). The particular data used for this table is described later, in Section 2. Salinities at the outlet from San Francisco Bay (Fort Point; Fig. 1) are strongly related to both Sacramento and San Joaquin flows throughout much of the year. Flows in the two rivers, however, differ in how they correlate with the seasonal salinities from season to season (especially in the high-salinity summer and autumn seasons). For example, notice that summer salinities are strongly anti-correlated (−0.66) with summer San Joaquin River flows but weakly anti-correlated (−0.33) with summer Sacramento River flows. This difference in correlations arises because the San Joaquin River flows from a higher altitude, cooler, more snowmelt-dominated basin than the lower, warmer Sacramento River. Consequently, peak flows occur in the San Joaquin River when the snow melts in spring and summer, and more of the year's flow occurs in the summer months in the San Joaquin River than in the Sacramento. Thus the contribution of each river's flow variations to San Francisco Bay salinity variations is a function of its timing as well as of the amount of discharge that it contributes.

Notice, however, that winter salinities are almost as anti-correlated with *summer* flows in the San Joaquin River as with the winter flows. This counterintuitive relation is a result of the strong lag-correlation between the winter inflows to the Bay (that determine winter salinity) and the subsequent summer flows in the San Joaquin River. Temporal correlations between the Sacramento and San Joaquin River flows are shown in Table 2. The two rivers are moderately well correlated throughout the year, and indeed summer San Joaquin River flows are almost as correlated to spring (and winter) Sacramento River flows as to summer Sacramento River flows.

Thus the overall freshwater contributions of the various rivers to San Francisco Bay salinities are a complex mix of regionally shared and locally unique signals. The contributions are complicated by inter seasonal (lagged) correlations between the hydrographs of the various rivers. Consequently, attempts to understand the hydrologic and hydroclimatic influences upon seasonal salinity of San Francisco

Table 2
Correlations between Sacramento and San Joaquin River full natural flows, 1906–1992. Bold values—significantly different from zero at 99-percent level

San Joaquin flows	Sacramento River flows			
	Autumn	Winter	Spring	Summer
Autumn	**0.65**	0.28	0.21	0.22
Winter	**0.35**	**0.75**	**0.55**	**0.51**
Spring	0.30	**0.56**	**0.66**	**0.50**
Summer	0.19	**0.49**	**0.61**	**0.59**

Bay face several difficult questions: How much of a given season's salinity variation is due to concurrent flow variations in the various rivers? How much is due to flow variations in preceding seasons? To what extent do the correlations of streamflow in the rivers of the western Sierra Nevada with salinity variability in the Bay arise from river-to-river and season-to-season flow correlations, rather than from direct responses of salinity to the flow variations in a particular river in a particular season?

1.2. Scope

In an effort to better understand the contributions of the rivers of the Sierra Nevada during different seasons to salinity variations in San Francisco Bay, in order to provide a better perspective as to which Sierra Nevada rivers are most important to San Francisco Bay salinities when, we have analyzed all the interseasonal streamflow correlations for the eight major rivers discharging from the western Sierra Nevada. This improved perspective on when various rivers are more (or less) influential may provide a sounder basis for allocating research efforts among Sierra Nevada rivers in the interests of improved management of the Bay ecosystems. The challenges of disentangling interseasonal correlations in hydrologic sequences are not uncommon, and the methods used here provide one approach to addressing them. In this study, an extended empirical orthogonal function (E-EOF; Weare and Nasstrom, 1982) analysis was performed on seasonal hydrographs of the eight major Sierran rivers. This analysis identifies distinct (uncorrelated) modes that streamflow from the Sierra has historically assumed and provides a disentangled description of the influences of (and on) those modes. Section 2 describes the data used and the E-EOF-analysis method. Sections 3 and 4 describe analyses of runoff and flow variations along the western Sierra Nevada. Correlations between variations in runoff (streamflow per unit area) and climatological conditions are used to identify the primary climatic forces driving runoff generation. Then, correlations between variations in streamflow and salinity variations in San Francisco Bay are used to determine which rivers influence salinity most each season. Results are discussed and summarized in Section 5.

2. Methods

The raw materials for the present analysis are monthly full-natural flows from the eight major rivers that drain from the Sierra Nevada through San Francisco Bay. Monthly reconstructions of these flows for each of the eight rivers are provided by the California Department of Water Resources (State of California, 1986), and are available since 1906. Full-natural flow is a reconstruction of the flow—above the first major reservoir (in most cases) and below where the last Sierra Nevadan flow contributions enter a river—that would have occurred if diversions and reservoir storage had not interfered, but still including current riparian and other water uses. It is a best available long-term estimate of the flow rates under 'natural' conditions. The full-natural flows of the Sacramento and San Joaquin Rivers, analyzed here, are for gages in the upper reaches of these rivers prior to their confluences with the other rivers analyzed. The monthly values provided by the Department of Water Resources were summed and centered (by subtracting the long-term means for each season and river) to form seasonal anomalies for October–December, January–March, April–June, and July–September from 1906 to 1992. Similar analyses were made using the original monthly time series, but resulted in a much more complex presentation that, although providing the same conclusions, was less suited for presentation in a short paper. The seasons analyzed here are shifted from the 'climate' seasons (September–November, December–February, and so forth) to better capture the seasonal character Sierra Nevada runoff variations (as in Aguado et al., 1993; Cayan et al., 1993).

The flow anomalies were analyzed in two forms. Because the hydrologic–hydroclimatic processes are better elucidated by considering both the runoff rates (defined here as the total flow divided by the basin area) and the total flow volumes, this paper addresses full-natural flows divided by the basin areas in Section 3. However, because salinity in San Francisco Bay responds to overall flows from the various rivers, the total flows must also be considered. In Section 4, therefore, the influences of the flow-volume anomalies are analyzed.

Freshwater inflows to the Bay are modified by a large number of water users and structures arrayed

upstream from the Delta into the Sierra Nevada and, thus, an important part of the freshwater-inflow variability experienced by the Bay is neglected here. However, recent studies (Knowles, 2000, 2002; Stahle et al., 2001) show that upstream management modifies the details of those inflows but changes its year-to-year character less than might be expected. Our interests here are to better understand the linkages from climatic forcings to Bay salinities as mediated by the spatially and temporally correlated freshwater flows from various parts of the Sierra Nevada. The connections of streamflow variations to climate variations are most clearly represented (at present) by the full-natural flows, and salinities frequently reflect, in a complex fashion, the natural flow fluctuations, especially in extremely wet and dry years which dictate much of the correlation structure of the flow and salinity series (Knowles, 2002), excepting, most notably, some long term trends in salinity (Peterson et al., 1995; Stahle et al., 2001). Finally, the interactions between salinity and full-natural flows have been complicated, and the two have been artificially intertwined, by salinity management practices now in place that vary the salinity standards that must be met by streamflow management according to full-natural, rather than managed, flow totals from the eight rivers (California Department of Water Resources, 2000). Thus, the use of full-natural flows throughout this paper represents a somewhat uneasy compromise in the interests of brevity.

The relative sizes of the eight rivers, and some of their relative importance in the analyses that follow, differ depending on whether runoff or total flow is considered. For example, the middle-altitude, central Sierra Nevada yield more runoff per square kilometer, and more runoff variability, than do either the low-altitude basins of the northern Sierra Nevada and parts of surrounding ranges (e.g. the Sacramento) or the high-altitude basins of the southern Sierra Nevada (e.g. the San Joaquin), as shown in Fig. 2. The Yuba River has the largest mean and standard deviation of runoff (except in summer) followed by the nearby American River. The Sacramento and San Joaquin Rivers have the smallest mean and standard deviations of runoff per unit area in most seasons. In terms of total flows, however, because it is a much larger basin than the others (Fig. 1), the Sacramento River has the largest mean and standard deviations. The Merced River and the other smaller basins in the southern Sierra Nevada yield the least total flows and flow variabilities.

A steady progression of streamflow seasonality also is evident in Fig. 2 from the low-altitude, rainfall-runoff dominated Sacramento River in the north toward more snowmelt dominance in the flow and runoff hydrographs in the higher, southern parts of the Sierra. The peak runoff seasons are winter in the Sacramento River, winter and spring in the Feather, Yuba, and American Rivers, and spring in the Stanislaus, Tuolumne, and Merced Rivers. The San Joaquin River has a spring-into-summer runoff peak.

Two long-term measures of salinity in San Francisco Bay and several measures of local and regional climatic conditions were compiled for comparison with the seasonal totals of full-natural flow in the rivers. Centered seasonal averages were computed from long-term salinity series at Fort Point near the mouth of San Francisco Bay, 1922–1989, and at Alameda in the center of the estuary, 1940–85 (Fig. 1). Arguably, autocorrelations in these salinity series could have been removed by prewhitening; however, for consistency with the rest of the analysis presented here, which is explicitly designed to maintain the information in the seasonal autocorrelations of various flow, meteorological, and salinity series, no prewhitening of the salinity was performed here.

Noting that precipitation and, especially, temperature have broad regional coherence, a single regional time series of each was judged adequate for our diagnostic purposes. Regional-average series of precipitation and temperature were constructed from four Sierra Nevada weather stations, 1931–1992 (described in Dettinger and Cayan, 1995); the autocorrelation structures of these series will be discussed in a later section. Regional atmospheric-circulation conditions are illustrated by an index of sea-level pressures in a region near and over California that has been shown to be anticorrelated with California precipitation—the California Pressure Anomaly (CPA, defined in Cayan and Peterson, 1989); in this study, the CPA from 1907–1992 will be compared to the runoff variations to understand their atmospheric forcings. Two even larger scale indices that are often useful in describing

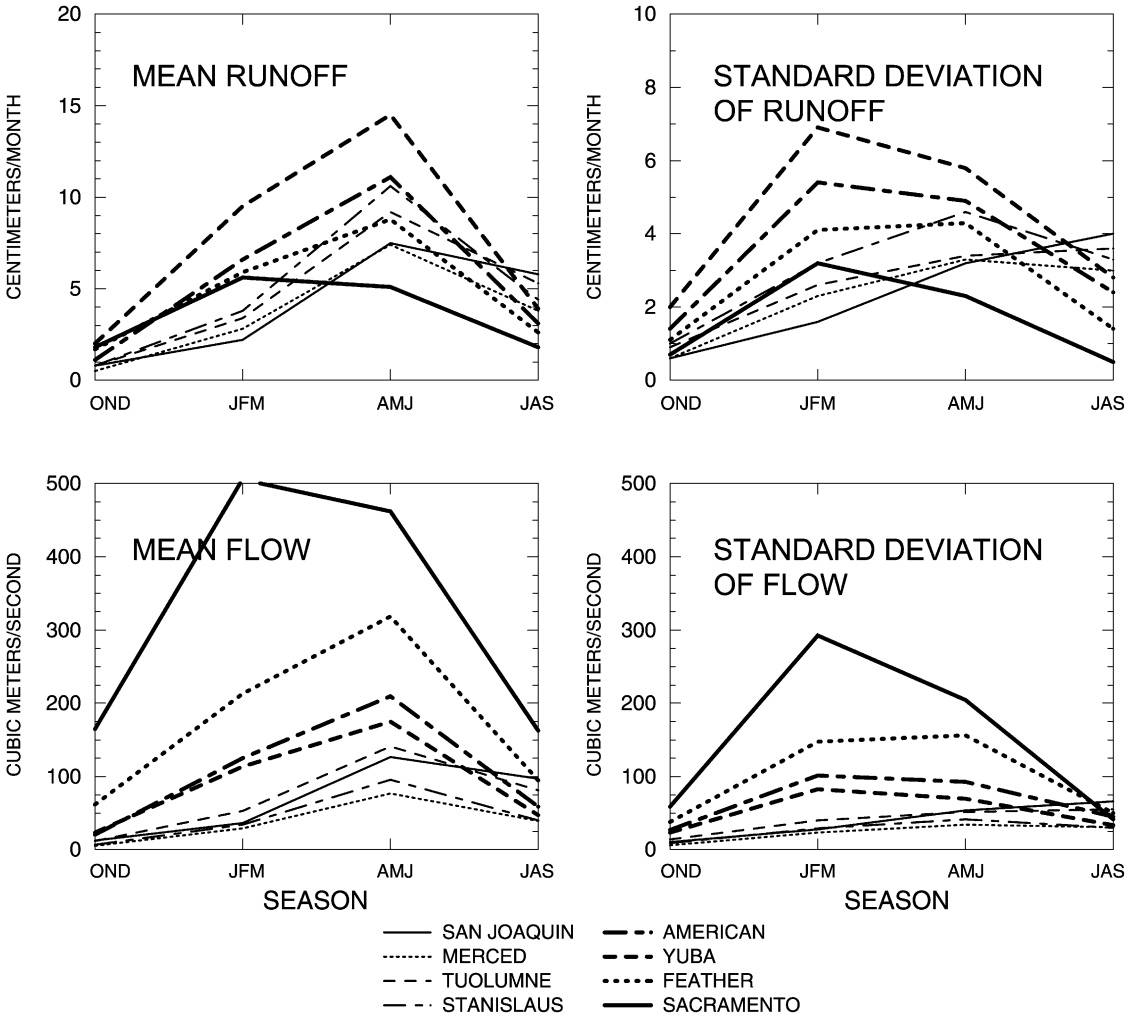

Fig. 2. Seasonal means and standard deviations of runoff and flows of Sierra Nevada rivers, 1906–1992.

the hydroclimatology of the western states are the Southern Oscillation Index (SOI)—an index of the El Niño climatic oscillation of the Tropical Pacific Ocean region (e.g. Philander, 1990; Cayan and Webb, 1993) and the Pacific-North American index (PNA)—an index of north–south excursions of wind patterns over the North Pacific and North American sectors (Leather et al., 1991). Correlations between these various hydroclimatic/salinity series and several distinct components of streamflow variability in the Sierra Nevada were computed to help identify the most immediate and likely causes of the various streamflow modes.

To extract distinct (uncorrelated) modes of seasonal streamflow variability, the centered runoff and flow series were subjected to an E-EOF analysis (Weare and Nasstrom, 1982). E-EOF analysis is a form of principal component analysis (PCA) designed specifically to extract principal modes of variability that yield the interwoven spatial cross correlations and temporal lag correlations in a collection of time series. By E-EOF, a parsimonious set of distinct patterns of seasonal streamflow variation (at seasonal lags) among the eight rivers is identified. The modes are, by construction, distinct in that the patterns described are uncorrelated with each other and in that the time

series that measure the occurrence of these patterns in the original time series are uncorrelated in time. This doubly uncorrelated description of the streamflow variations ensures that influences on, and by, the streamflow variations can be analyzed without any double accounting. The modes are parsimonious in that, by construction, they also describe the largest fractions of overall streamflow variance with the fewest uncorrelated time series. In the present analysis, a complete description of almost 90% of the variance in the yearly seasonal cycles in the eight rivers (amounting to essentially 32 intercorrelated time series) is reduced to just three uncorrelated time series. The E-EOF description of the streamflow variations is complete in that, if all 32 E-EOFs were analyzed, none of the original streamflow variations would have been discarded. That is, the original time series from all the rivers can be reconstructed in their entirety from the full set of E-EOFs. This completeness is an advantage of the E-EOF analysis compared to more standard approaches to lag correlated time series such as prewhitening. Prewhitening treats lag correlations as defects, limitations, of the time series being analyzed and discards the lag correlations as a first step in analysis. The lag correlations, however, are important characteristics of the series considered here and their influences are what motivated this analysis (as discussed in Section 1). Indeed, E-EOF analysis was chosen for use here specifically because it is designed to accommodate and describe the lag correlations and spatial correlations in a natural way without discarding either.

E-EOF analysis is a form of PCA, which—in applications like this—is an analysis of the instantaneous spatial cross correlations among time series that extracts the most influential modes of spatially shared variations. E-EOF analysis is an augmentation of PCA to address both the instantaneous correlations analyzed by PCA and a limited number of time-lagged correlations among all the series (in this case, a full year's worth of lags). By this augmentation, E-EOF analysis addresses temporal and spatial correlations together in the same way that PCA analyzes the spatial correlations alone. E-EOF analysis describes spatial cross correlations and temporal lag correlations simultaneously in a self-consistent way to identify (in this case) the principal components of annual cycles of lag- and spatial-cross correlations in and among the flow series from the eight rivers that drain to San Francisco Bay.

The E-EOF analysis proceeded as follows: eigenvectors were computed for the cross-covariance matrix, Z^tZ, of a matrix, Z, of the eight flow (or runoff) series arranged like:

1906: {Autumn flow in river 1, autumn flow in river 2,…autumn flow in river 8, winter flow in river 1,…,summer flow in river 1,…,summer flow in river 8}
1907: {Autumn flow in river 1, autumn flow in river 2,…autumn flow in river 8,…,summer flow in river 1,…,summer flow in river 8}
...
...
1992: {Autumn flow in river 1, autumn flow in river 2,…autumn flow in river 8,…,summer flow in river 1,…,summer flow in river 8.}

Each row of Z is 32 elements wide (4 seasons × 8 rivers) so that the cross-covariance matrix is 32×32 and yields 32 eigenvectors. In a standard PCA, only the autumn flows would be included in the corresponding Z matrix, or else all seasons would be intermixed without regard for temporal order, to form a cross-covariance matrix that is only 8×8.

The eigenvectors, once divided by the sums of the squares of their elements (reducing each to a unit-length vector), are called E-EOFs (or—in the parlance of PCA—loadings; von Storch, 1995). The projections of each year's seasonal flows (or runoff rates) onto these E-EOFs are the principal-component (PC) series (or amplitudes). The leading E-EOFs can be interpreted as normalized depictions of the distinct (uncorrelated) and most common modes of season-to-season runoff variation in the overall data set. The PC series are the year-to-year history of strengths of the particular modes described by the E-EOFs. The eigenproblem solved is such that the E-EOFs are mutually independent (orthogonal) and the PC series that describe their year-to-year strengths are uncorrelated with each other. The E-EOFs that represent the most flow variance overall and their corresponding PC series provide an economical set of indices that can be used to describe the ways that runoff and flow totals from the Sierra Nevada have varied historically in the most concise way.

To identify the dominant hydroclimatic forcings of these independent runoff modes and the salinity responses to them, simple linear correlation coefficients were computed between the PCs and seasonal salinity, precipitation, temperature, and atmospheric-circulation series. Because the PC time series correspond to distinct modes that are temporally uncorrelated with each other, they allow no double-accounting of variability. As such, they provide the opportunity to consider the influences on streamflow, and the influences of streamflow, without the confounding effects of the strong cross correlations in Table 2. Because the E-EOF analysis performed here addresses variations throughout the annual cycle simultaneously, the confounding lag correlations are handled transparently.

Finally, the E-EOFs were rotated by the orthogonal Varimax scheme (Richman, 1986) in an attempt to develop the most 'realistic' flow groupings and to more completely isolate the contributions of the seasonal climatic forcings and to the seasonal salinities. Rotation is an optimization scheme that (as applied here) maximizes the range of magnitudes of the weights in each rotated EOF (R-EOF) while maintaining uncorrelated strengths (R-PC series). The procedure is such that the resulting PC time series remained uncorrelated with each other, but the constraint (implicit in the original EOF computations) that E-EOFs be orthogonal was relaxed. Whether to analyze the unrotated or rotated EOFs is arguable (e.g. Legates, 1991, 1993; Richman, 1993). Neither is entirely satisfactory to describe all of the runoff variability but, in the interests of brevity, only the rotated EOFs will be described in detail. Seasonal components of the annual hydrographs are separated almost completely in the R-EOFs, which is useful for understanding the particular contributions of the individual seasons.

3. Runoff variations and hydroclimatic forcing

The E-EOF analysis provides a parsimonious and seasonally disentangled description of the eight runoff series. The most parsimonious set of E-EOFs is identified by considering the contributions that each makes to the overall runoff variance. A reasonable tradeoff between analyzing enough E-EOFs to describe as much runoff variability as possible, while using the fewest number of E-EOFs (to simplify both the subsequent analysis and presentation) is found by looking for a point of diminishing returns in the (sorted) percentages of variance captured by each E-EOF, shown in Fig. 3. The first three E-EOFs describe much more variance than any (or all) of the remaining E-EOFs and thus using more than those three yields diminishing returns. Alternatively, the statistical significance of the E-EOFs can be considered. The statistical significance of EOFs is commonly judged by the contributions that they make to the overall variance of the time series analyzed and, in particular, the extent to which those variance contributions differ from the 'noise ramp' of variances from the EOFs making the smallest contributions. This difference is typically judged by looking for a break in slope of the variance contributions when they are plotted as in Fig. 3 (log variance versus eigenvector number; North et al., 1982). In Fig. 3, however, although there are notable breaks in the slope of the curve at about the third and eighth eigenvectors, only the first three eigenvectors contribute more than Guttmann's (1954) lower bound on factor significance—which is the percent of variance that would be captured from white noise by a purely random EOF. This lower bound is (total variance)/(total number of E-EOFs) and, in Fig. 3, is (100 percent)/(32 E-EOFs) or 3 percent. Only the first 3 E-EOFs contribute more than this bound. Therefore, only the first 3 PC series will be considered further.

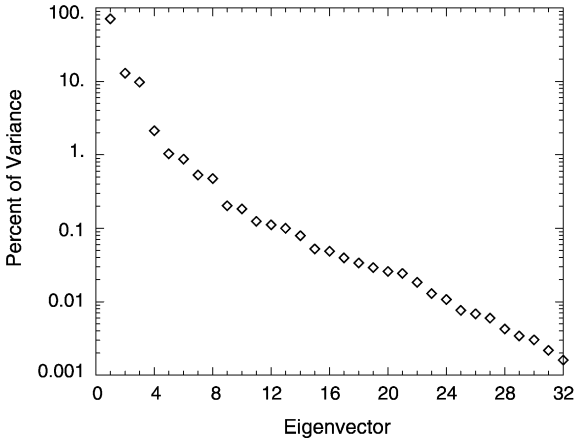

Fig. 3. Percent of variance of seasonal Sierra Nevada runoff rates captured by each E-EOF, 1906–1992.

These three E-EOFs together capture 86 percent of all the variability in the seasonal runoffs of the combined eight rivers. Thus we can reduce the description of four seasons of runoff per year in eight different, but strongly correlated, rivers to the analysis of only three uncorrelated and annual time series, with only a 16% loss in resolution, by using E-EOF analysis.

In order to simplify matters still further, the leading 3 E-EOFs and PCs were rotated according to a Varimax optimization in S-mode (Richman, 1986). Notably the same variability captured by the 3 unrotated E-EOFs is still present in the rotated E-EOF/rotated PC combinations. It has simply been separated differently in the unrotated and rotated results. In the present analysis, the result of S-mode rotation was a set of R-EOFs that had only positive weights. Each R-EOF is shown in Fig. 4 as a series of seasonal 'hydrographs' with weights that vary from river to river and seasonal to season. The similarities of these 'weighting hydrographs' to the actual hydrographs of the eight rivers in a given year are measured in the R-PC series (Fig. 5).

The value of rotation, in this case, comes from its ability to separate seasonal influences. The leading 3 unrotated E-EOFs of runoff (not shown here) describe the 8 hydrographs in terms of a mode of year-to-year flow variations that are shared by all 8 rivers (63% of variance), a mode describing warm-season to cool-season shifts in runoff timing (14%), and an autumn flow mode (11%). In contrast, the R-EOFs provide relatively simple separations between winter, spring, and autumn runoff variations that are as clear as possible while—by design—being uncorrelated with each other on the annual time scale. Although the separation looks simple, the EOF analysis ensures that the weights correctly reflect the relative importance in the various river of each mode (season) and that the influences of, and the influences on, the year-to-year variations in strength of each mode can be considered entirely independently from the others.

The first R-EOF emphasizes runoff variations in the spring, except in the Sacramento River. The spring runoff contributions to R-EOF 1 derive mostly from the middle-altitude central Sierra Nevada rivers and also from the high, snowbound southern Sierra Nevada rivers. The second R-EOF is dominated by winter-runoff weightings. Again, the highly productive central Sierran rivers are weighted most.

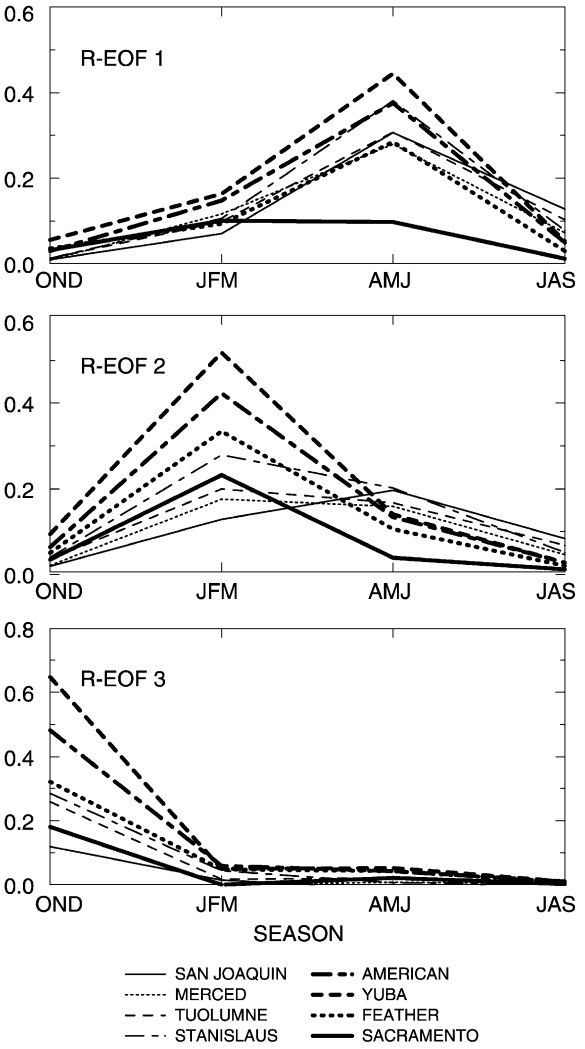

Fig. 4. Rotated extended EOFs of seasonal runoff from eight Sierra Nevada rivers.

Notably, spring runoff in the snowbound southern Sierran river basins (San Joaquin, Merced, Tuolumne, and Stanislaus) is weighted almost as much or more than winter runoff in this mode. Thus R-EOF 1 reflects those parts of the hydroclimatology that are 'everywhere' destined to yield spring runoff whereas R-EOF 2 is more associated with hydroclimatology that consistently affects winter runoff and that may or may not yield spring runoff depending on the year and river. The third R-EOF captures autumn runoff variability. Weights are largest for autumn Yuba

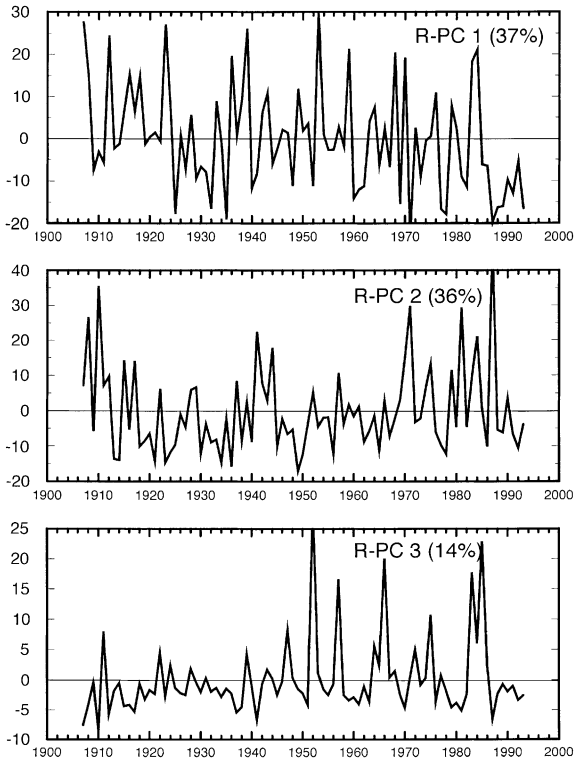

Fig. 5. Rotated extended principal-component series of seasonal runoff from eight Sierra Nevada rivers. Percentage of variance captured by each component is shown in parentheses.

and American runoff, and the weights for Sacramento and San Joaquin River runoff are smallest.

The first R-PC (reflecting springtime runoff) reflects drought/wet years, with sustained or deep negative values in the drought years around 1930, in 1976–1977, and 1987–92 (Fig. 5). In contrast, positive values are notable for wet years like 1969 and 1983. The second R-PC (reflecting winter runoff) also has strong wet-year signals but with more of an emphasis on the warm-wet winters—years with early runoff peaks like 1986—than R-PC 1 (Fig. 5). That is, different wet years are emphasized by R-PC 1 versus R-PC 2. R-PC 2 is especially prominent during the wet spell of the late 1970s and early 1980s when high flows in winter were common. Notably also, the recent 1987–1992 drought is less evident in the winter-flow mode (R-PC 2) than in the spring-flow mode (R-PC 1).

There are hints of a trend in recent halves of both R-PC 1 (negative) and 2 (positive). Together these weak trends describe a highly significant recent trend toward earlier snowmelt and streamflow in California (Dettinger and Cayan, 1995; Peterson et al., 1995; Cayan et al., 2001). The trend has been split between the two R-PCs and is masked by other variability, but was quite clear in the unrotated PC 2 (not shown) with a trend significant at $p = 0.005$ by a Kendall's tau trend test (Press et al., 1989). The unrotated PC 2 captured (with nearly balanced positive winter weights and negative spring and summer weights) shifts from warm-season toward cool-season runoff. As with R-PCs 1 and 2, the unrotated PC 2 was weighted more upon the central Sierran rivers. Thus, the recent runoff trend has been more influential in the middle-altitude basins of the central Sierra Nevada than in either the warmer northern Sierran rivers or the frigid southern rivers—in keeping with the findings of Dettinger and Cayan (1995) and Jeton et al. (1996).

The third R-PC (autumn mode) is notable for its tendency to be composed of small fluctuations around zero with a few large positive excursions. This behavior reflects the fact that autumn runoff from these rivers is usually small and frequently little more than base flow. Thus, autumn runoff is near its natural lower limit and does not decrease much even in dry years. During years with unusually wet autumns, however, runoff rates *can* increase and large positive spikes in R-PC 3 arise.

The relations of these R-PCs to historical precipitation and temperature variations clarify the climatic underpinnings of each season's (mode's) runoff variations. The springtime runoff mode (R-PC 1) is correlated with a broad combination of autumn, winter and spring precipitation totals and (negatively) with winter and spring temperatures (Table 3), reflecting direct contributions to springtime flow from each season's precipitation and the tendency of warm winters and springs to yield more winter snowmelt and runoff. Some of the negative correlation between spring temperature and R-PC 1 also may result from the strong negative correlation between spring precipitation and temperature in the Sierra ($r = -0.69$). In contrast, temperature and precipitation in the Sierra Nevada in winter and summer seasons are, at most, modestly (negatively) correlated. Furthermore, all interseasonal combinations of precipitation and temperature are poorly correlated, with the exception of a significantly positive correlation

Table 3
Correlations between R-PCs of runoff and Central Sierra precipitation totals and temperatures, 1931–91. Bold values—significantly different from zero at 99-percent level

	Previous summer (July–September)	Autumn (October–December)	Winter (January–March)	Spring (April–June)	Summer (July–September)
Runoff R-PC	Precipitation totals				
1 (spring)	−0.21	**+0.35**	**+0.46**	**+0.53**	−0.01
2 (winter)	+0.10	**+0.33**	**+0.67**	−0.06	+0.28
3 (autumn)	−0.04	**+0.79**	−0.23	+0.14	+0.16
Runoff R-PC	Mean temperature				
1 (spring)	−0.17	−0.31	**−0.52**	**−0.49**	−0.12
2 (winter)	+0.00	+0.03	**+0.48**	+0.08	−0.22
3 (autumn)	−0.10	+0.06	−0.01	−0.11	−0.14

between spring and summer temperatures ($r = 0.35$, $p \sim 0.001$). Thus, most possible combinations of seasonal precipitation and temperature can be viewed as essentially independent forcings when interpreting Table 3.

The winter runoff mode (R-PC 2) is almost exclusively a function of winter precipitation and temperature. Thus spring runoff from the Sierra Nevada integrates much more of each year's hydroclimatic variation than does winter runoff. Cayan and Peterson (1993) and Aguado et al. (1993) also have noted the critical role of spring temperatures and precipitation in determining flow timing in the Sierra Nevada. The autumn runoff mode (R-PC 3) is dominated by autumn precipitation. When correlated with monthly precipitation totals (not shown), R-PC 3 is more a reflection of November precipitation than either October or December; however, the positive spikes in R-PC 3 commonly reflect unusually wet Novembers *and* Decembers.

The seasonal precipitation totals and temperatures are, in turn, forced by large-scale climatic fluctuations that—in part—can be measured by a variety of simple atmospheric-circulation indices. The R-PCs developed here are, however, surprisingly uncorrelated with the 'traditional' atmospheric-circulation indices. To investigate such large-scale connections, correlations between the three R-PC series and the California Pressure Anomaly (CPA) index of Cayan and Peterson (1989), the SOI, and the PNA index were computed.

The CPA measures sea-level atmospheric pressure over, and offshore from, northern California. Low pressures in this region (which yield negative CPA values) are associated with the passage of storms and precipitation over the region. The CPA was specifically designed to be strongly anti-correlated with California precipitation totals (Cayan and Peterson, 1989) and is most anti-correlated with Sierra Nevada precipitation in autumn and winter ($r = -0.7$ for both). The winter runoff mode (R-PC 2) is anti-correlated with winter CPA (Table 4), which in turn is anti-correlated with winter precipitation. The winter-flow mode is also moderately anti-correlated with autumn CPA. In contrast, the spring-flow mode (R-PC 1) is essentially uncorrelated with the CPA (Table 4); some other atmospheric index more suited to diagnosing the combinations of both spring precipitation and cool-season temperatures would be needed to diagnose the springtime flows (Dettinger and Cayan, 1992). Notably, neither the SOI nor the PNA meets this need in a consistent manner for the Sierra Nevada, because the Sierra Nevada (1) straddles the line separating southwestern regions with wetter-than-normal El Niños (indexed by SOI) from northwestern regions with drier-than-normal El Niños (e.g. Cayan and Webb, 1993; Dettinger et al., 1998), and (2) straddles the line separating regions with warmer-than-normal and cooler-than-normal conditions associated with particular phases of the PNA (Leather et al., 1991). Only the winter PNA (Table 4) is significantly correlated to one of the R-PCs, and that relation is to the winter runoff mode (R-PC 2). The SOI (not shown) is even less correlated to the R-PCs. The relations between the springtime runoff mode—as delineated here—and the seasonal circulation

Table 4
Correlations between R-PCs of runoff and California Pressure Anomaly, 1907–92, and Pacific North American index, 1946–84. Bold values—significantly different from zero at 99-percent level

	Previous summer (July–September)	Autumn (October–December)	Winter (January–March)	Spring (April–June)	Summer (July–September)
Runoff R-PC	California Pressure Anomaly				
1 (spring)	+0.21	−0.06	−0.21	−0.06	+0.01
2 (winter)	−0.17	**−0.34**	**−0.58**	+0.12	+0.18
3 (autumn)	+0.16	**−0.49**	+0.21	+0.11	−0.10
Runoff R-PC	Pacific-North America Index				
1 (spring)	−0.05	−0.21	−0.06	+0.02	+0.06
2 (winter)	+0.16	+0.36	**+0.42**	−0.04	+0.20
3 (autumn)	−0.03	−0.12	+0.05	+0.00	−0.29

indices are further complicated because the spring runoff mode is a function of a much longer interval of climatic forcings within each year than is the wintertime mode and this spreads the forcings (and correlations) over several seasons, leaving none well correlated. The autumn-flow mode (R-PC 3) is moderately anti-correlated with autumn CPA (which in turn is anti-correlated with autumn precipitation). The generally modest correlations between the R-PCs and CPA indicate that, at the level considered here (river-to-river and season-to-season variations), large-scale controls on precipitation are only part of the story. Temperature variations, other climate variations not captured by the simple CPA, and local weather fluctuations play at least as great a role.

4. Full-natural flows and San Francisco Bay salinities

Salinity of San Francisco Bay decreases with increases in freshwater inflow from the Sierra Nevada as the inflows flush salt water from much of the estuary, and it increases when freshwater inflows decline. The flushing depends on the total freshwater flow into the Bay and not (as much) on per-unit-area rates of runoff generation in various river basins. Thus, in order to understand the connections between runoff in the Sierra Nevada and salinity in San Francisco Bay, the streamflow volumes from the rivers must be analyzed. In this study, full-natural flow estimates are used, to avoid complications due to human management of the water resources (management that modifies flows both at the major reservoirs on each river and, in the valleys, below where the rivers have merged). This approach also maintains the strongest ties to the climatic forcings discussed in Section 3. Notably, Knowles (2002) and Stahle et al. (2001) show that, although Bay salinities are significantly affected by upstream management of the rivers (e.g. Peterson et al., 1995), the natural, hydroclimatically driven variations of those rivers (as indexed by full-natural flows and by tree-ring reconstructions of the flows) are still the dominant feature of year-to-year salinity variations.

E-EOF analysis of the variability of all eight streamflow series (not shown here) tended to be dominated by the variability of Sacramento River flows because that river basin is much larger (25,000 km^2) than the rest (2500–10,000 km^2) and has greater absolute variability than any one of the other rivers (Fig. 2). Together, though, the other river basins are larger than the Sacramento River basin and exhibit more overall variance (Figs. 1 and 2). Furthermore, Fig. 4 and, especially, Fig. 2 indicate that the annual cycles of flow and flow variation in the Sacramento River are quite different from those in the other rivers. Sacramento River flow is more concentrated in winter. When flows in the eight rivers were analyzed as eight separate rivers, the large volume of the Sacramento River, and its winter-dominated seasonal cycle, forced E-EOF of flows to focus preferentially on winter responses.

A more balanced analysis of the flows was provided when the flows of the central Sierra Nevada were summed, and the flows of the southern Sierra

were summed, so that three more nearly equal flow series (Sacramento, central Sierra, and southern Sierra) were analyzed. The observation that three E-EOFs are significant in the E-EOF analyses of runoff rates and in the analysis of flows in all eight rivers (not shown) indicates that there are essentially only three degrees of freedom in the combined seasonal hydrographs of the major Sierra Nevada rivers. Also, inspection of Fig. 2, and the E-EOFs of runoff in the eight rivers (not shown here), confirmed that the Sacramento River flow hydrograph is distinct in its timing from those of the central Sierran rivers (Feather, Yuba, and American Rivers) which in turn are different from those of the southern Sierra Nevada (Stanislaus, Tuolumne, Merced, and San Joaquin Rivers). These clusters are largely dictated by differences in streamflow timing due to increases in basin altitudes and coolness as one progresses from the Sacramento River basin (north) to the San Joaquin River basin (south). These three 'clusters' of rivers drain roughly similar total areas: southern Sierra rivers, 14,000 km^2; central Sierra rivers, 19,000 km^2; and Sacramento River, 25,000 km^2. Therefore, the E-EOF analysis of these grouped flow totals are used here to unravel the variations that drive San Francisco Bay salinities, although similar results were obtained when various less-obvious normalizations of the 8 flow series were analyzed instead.

The leading three E-EOFs from analysis of the grouped full-natural flows capture 94 percent of the overall variability, and each of the three contributed more than Guttman's lower bound on eigenvalue significance (100 percent/(4 seasons × 3 groups)). Therefore, as in the runoff analysis, the three leading modes are considered further. The unrotated E-EOFs and their PCs were analyzed and then rotated by the same orthogonal S-mode Varimax method used in the runoff analysis. For brevity, only the rotated E-EOFs (designated FR-EOFs for flow R-EOFs) and FR-PCs are presented here.

As in the runoff analysis, the FR-EOFs describe distinct seasons of flow. The first FR-EOF mostly represents winter flows with most weight on the central Sierra and Sacramento flows (Fig. 6). Least weight is given to the southern Sierra flow. The second FR-EOF is dominated by springtime flows, with maximum weight on the central Sierran flow and least on the Sacramento River flow. The third FR-EOF

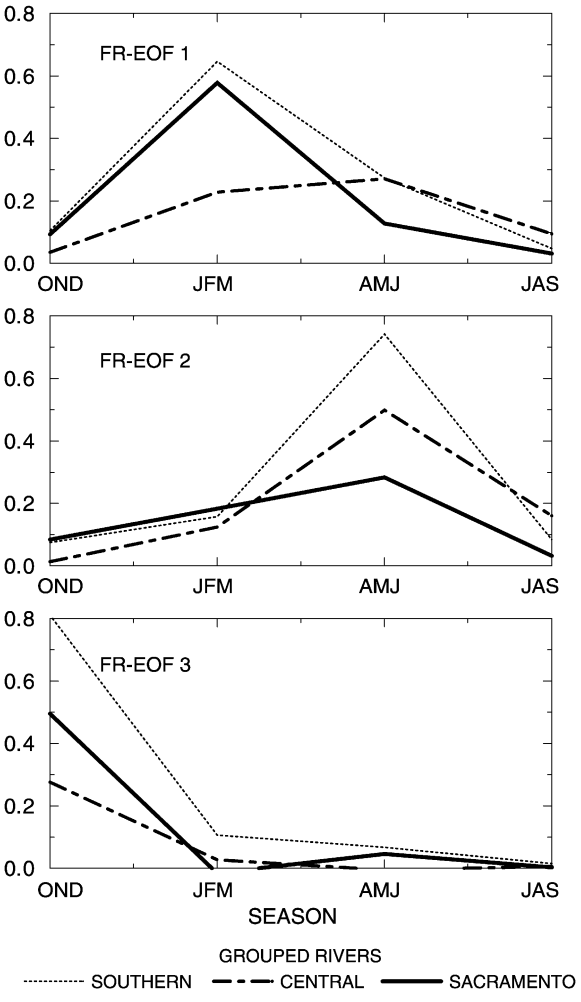

Fig. 6. Rotated extended EOFs of seasonal, grouped full-natural flows from the western Sierra Nevada.

reflects autumn flows almost exclusively and the central Sierra flow is weighted most (again) followed by Sacramento River flow. These FR-EOFs indicate that, among the grouped flows, winter flow variability is concentrated in the central and Sacramento rivers, spring flow variability is concentrated in the central and southern rivers, and autumn flow variability is concentrated in the central and Sacramento Rivers. Flow from the central Sierra Nevada is important in all three modes because its flows are a combination of autumn and winter rainfall-runoff and spring snowmelt, due to its middle-altitude basins. The Sacramento River flow is important in winter and autumn

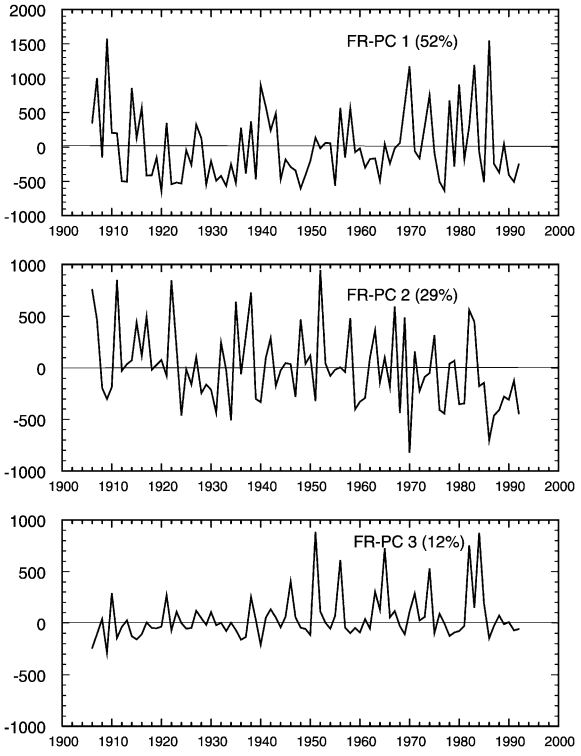

Fig. 7. Rotated extended principal-component series of seasonal, grouped full-natural flows from the Sierra Nevada. Percentage of variance captured by each component is shown in parentheses.

flow because its basin is low and warm and flow peaks early. The southern Sierra basins are at higher altitudes and cooler than the rest, are more snowmelt driven, and thus are primarily influential in spring and summer.

The three leading FR-PCs (Fig. 7) are strongly related to the runoff R-PCs corresponding to the same flow seasons. The winter-flow mode (FR-PC 1) variations are very similar to the second R-PC mode of runoff ($r = -0.96$), the spring-flow mode (FR-PC 2) is similar to the first R-PC ($r = -0.98$), and the autumn-flow mode (FR-PC 3) is similar to the third R-PC ($r = -0.98$). Thus the correlations between these flow-PC series and seasonal precipitation and temperature (not shown) are similar to those in Table 3. When aggregated to the scale of the three groups of rivers considered in this section, runoff rates and streamflows respond together to climatic variations; in contrast, when analyzed river-by-river, the Sacramento River flow dominated the results and skewed them more towards winter forcings and responses.

Responses of salinity in San Francisco Bay to these various modes of streamflow are described here in terms of long monthly salinity records from two sites. Fort Point is located just outside the mouth of the estuary, north of the Golden Gate (Fig. 1), and salinity there reflects the degree of freshwater flushing of the Bay and salinities in the coastal ocean. Salinity in the Fort Point record typically shows a slower response to Delta inflows to the Bay than other locations farther up the estuary (Peterson et al., 1989). This salinity record is used because of its long period of record (serially complete throughout the interval 1922–present). Alameda is located within the estuary near the juncture of the mouth, northern, and southern parts of the Bay, near where water converges from the coastal ocean, the Delta-inflow-dominated North Bay, the sluggish, local inflow- and evaporation-influenced South Bay (Peterson, 1995). Alameda has a shorter and less complete record of salinities than Fort Point, but does encompass over 4 decades with ample variability.

All correlations of salinity at both sites with the flow modes are negative (Table 5)—because larger freshwater flows into the Bay reduce salinity within, and at the outlet of, the Bay almost regardless of when they occur. Autumn salinities at both sites are strongly anti-correlated with the autumn-flow mode (FR-PC 3) and moderately with the previous year's winter- and spring-flow modes (FR-PCs 1 and 2). Recall that FR-PC 3 is characterized by small fluctuations in most years punctuated by a few large positive excursions, especially since the 1940s. Autumn salinities at both sites also display this erratic behavior in the most pronounced autumn-flow years (notably, water years 1951 and 1984) but do not respond as much in other years. For example, if water years 1951 and 1984 are removed from the calculation, the Fort Point anti-correlation drops from -0.67 to -0.44, and if all years with FR-PC 3 > 250 are removed, the correlation—between the variations in near-normal years—is -0.48 overall. Thus autumn-flow excursions must be among the largest on record to cause a significant seasonal salinity response at Alameda and Fort Point. The FR-PC 3 correlations with autumn salinities indicate that autumn salinity is most

Table 5
Correlations between FR-PCs of grouped eight-rivers flows and salinity at Fort Point, 1922–89, and at Alameda, 1940–85. Bold values—significantly different from zero at 99-percent level

	Autumn (October–December)	Winter (January–March)	Spring (April–June)	Summer (July–September)	Next Autumn (October–December)
Flow FR-PC	Mean salinity at Fort Point				
1 (winter)	−0.21	**−0.73**	−0.28	−0.29	**−0.37**
2 (spring)	−0.17	**−0.40**	**−0.76**	**−0.74**	**−0.47**
3 (autumn)	**−0.63**	−0.30	−0.05	−0.20	−0.23
Flow FR-PC	Mean salinity at Alameda				
1 (winter)	−0.14	**−0.82**	**−0.58**	**−0.54**	**−0.43**
2 (spring)	−0.13	−0.29	**−0.66**	**−0.75**	**−0.41**
3 (autumn)	**−0.67**	**−0.36**	−0.14	−0.25	−0.25

dependent upon variations in autumn flows from the central Sierra Nevada and the Sacramento River.

Early autumn salinity is the maximum of the annual cycle and imposes some of the most severe salinity stresses on the Bay's ecosystems. Salinities in the winter and spring seasons, however, also have important biological implications and thus are the crucial indicators for the Bay ecosystem (e.g. Jassby et al., 1995). Winter salinities at both sites are most strongly anti-correlated with the 'winter-flow' mode (FR-PC 1). Minor correlations of Fort Point salinity with the spring-flow mode (FR-PC 2) and of Alameda salinity with the autumn-flow mode (FR-PC 3) are found (Table 5). These correlations indicate that the wintertime salinity variations are mostly imposed by the large winter-to-winter excursions in rates of early runoff and streamflow from the Sierra Nevada. Wintertime salinity has little memory because it is faced with a concurrent flow variability of such great magnitude relative to the preceding seasons. Although not shown in Table 5, correlations between salinity and each of these FR-PCs drop essentially to zero by the following winter (despite the moderate 'next autumn' correlations). Thus, the large winter flow variations overwhelm all antecedent influences on salinity anomalies. These winter flow variations are largely a near-equal mix of variations from the central Sierra and Sacramento River (Fig. 6).

Variations of the spring-flow mode (FR-PC 2) result in corresponding (negatively correlated) spring and summer salinity variations at both sites. At Fort Point, FR-PC 2 is also moderately correlated to winter and next-autumn salinities. At Alameda, spring and summer salinities also are well correlated to FR-PC 1 (the winter-flow mode). The spring FR-EOF 2 flow mode has the longest influence on San Francisco Bay salinities overall but at Alameda, winter flows also continue to exert a strong influence well into the next autumn. The springtime-flow mode is dominated by the middle-altitude rivers of the central Sierra and the high-altitude rivers of the southern Sierra. The longer influence of these rivers on salinities presumably is a result of their later runoff peaks and the intraseasonal memory of climate imparted to those basins by the snowpacks that support much of their flows. As indicated previously, FR-PC 2 components of flow are driven by winter and, especially, spring precipitation ($r = +0.34$ and $+0.55$, respectively) and by winter and spring temperatures ($r = -0.57$ and -0.52, respectively).

Alameda salinities apparently are more anti-correlated with large winter flows immediately and then retain the influence from those flows longer than do salinities at Fort Point. A similar pattern of strong concurrent and long-lasting lagged anti-correlations is suggested for the autumn-flow mode (FR-PC 3). The strong immediate response probably reflects Alameda's greater distance from the coastal ocean and its proximity to the northern part of the Bay where freshwater inflows from the Delta enter. The long memory of autumn and winter flows at Alameda may reflect its dependence on conditions both up- and down-estuary and the influence of the large and relatively sluggish hydrodynamics of the nearby southern arm of the Bay (Peterson, 1995).

5. Summary

In response to competing needs of San Francisco Bay ecosystems, upstream endangered species, and upstream water uses, salinity in the Bay during the February–June 'season' are managed to meet seasonal targets (Jassby et al., 1995; Peterson, 1995). These targets presumably will be met mostly through management of freshwater inflows to the Bay. Because of the large-scale hydroclimatic forcing shared amongst the various rivers that contribute inflow to the Bay estuary, the causes and effects of streamflow variations in the various rivers feeding the estuary can be difficult to separate. However, differences in runoff timing from river to river associated with different snowpack and snowmelt characteristics are in effect labels that allow us to sort out the runoff influences from the various contributing river basins. By separating the annual hydrographs for eight major rivers along the Sierra Nevada for each year from 1906–1992 according to sets of empirical, orthogonal (uncorrelated) functions that describe nearly all of the variability in the time series, shared components and river-to-river differences in runoff and flow fluctuations are readily visualized. By this approach, the sources and effects of natural runoff and streamflow variability in the San Francisco Bay's main freshwater-source region—the western slopes of the Sierra Nevada—are clarified in this paper. Full-natural flow estimates, and corresponding runoff rates (flow per unit area), for the upper San Joaquin, Merced, Tuolumne, Stanislaus, American, Yuba, Feather, and upper Sacramento Rivers (from south to north) are analyzed here.

Analysis of both runoff rates and full-natural flows indicates that almost 90 percent of the large-scale, year-to-year variations in flow from the western Sierra Nevada can be characterized in terms of three independently varying modes. The precise form of these modes is somewhat arbitrary and two different representations are shown here. Analysis of runoff from the eight river basins (that is, seasonal streamflows divided by basin areas) showed that overall about 63 percent of the annual variations is shared. The rotated EOFs of the runoff rates provided a separation of the runoff rates by individual seasons. Variations of winter- and spring-runoff modes contribute almost equally to the overall runoff variability along the western Sierra Nevada, followed by about half as much autumn contribution. In this analysis, summertime variability was distributed indistinctly among the other modes. In every season, variability of runoff from the central Sierra is dominant and variability of runoff from the Sacramento and San Joaquin River basins is smaller. Drought and wet years during the 1906–92 analysis period do not contribute equally to the modes, or even uniquely to any one of the modes; rather, the appearance of droughts and wet years in the various modes depends critically on winter and spring precipitation timing and temperatures. For example, the spring-runoff mode found here (R-PC 1) was more affected by the recent 1987–92 California drought than was the winter-runoff mode (R-PC 2). In contrast, the intense drought of 1976–77 was more consistently reflected in the winter-runoff mode. Part of this difference arises because springtime runoff (R-PC 1) is influenced by precipitation and temperatures over more of each year than is winter runoff (R-PC 2). A separate autumn-runoff mode (R-PC 3) was found and reflects the erratic nature of autumn flows in the Mediterranean climate of California; autumn runoff is either confined to a narrow range of low flows or else is large, depending mostly on whether precipitation arrives in a given autumn from one of the occasional large autumn storms or not.

Salinity variations in San Francisco Bay are driven by streamflow totals (m^3/s) rather than by runoff rates (mm/s). Thus the analysis was repeated for unnormalized full-natural flow estimates. The runoff analysis (as well as detailed analyses of all eight full-natural flows) indicated that rivers could be grouped into three sets based on shared seasonal distributions of flow. This grouping simplified the results of the flow analyses and gave more equal weighting to the various altitude zones and flow regimes of the Sierra Nevada. When flows were analyzed in terms of the sum of the flows in the four southernmost rivers, the three central rivers, and the Sacramento River, many of the results from the runoff analyses were almost directly transferable. Furthermore, correlation of the three dominant (seasonal) flow modes from this analysis with variations in San Francisco Bay salinity showed that autumn and winter salinities are mostly associated with concurrent flows (FR-PC 1 and 3, respectively). These flow modes are dominated by

the combined variability of the central Sierran rivers and the Sacramento River. Spring and summer salinities are dominated by a springtime-flow mode (FR-PC 2), which is mostly a function of the combined flows from the central and southern Sierra Nevada. This springtime flow mode responds to climatic forcings accumulated through much of the preceding year. Differences in salinity responses between Fort Point and Alameda suggest that, at this seasonal level, the interior of the estuary (Alameda) is more immediately and strongly affected by autumn and winter Delta inflows, and that due to its central location, the Alameda site also retains a stronger and longer lasting memory of those flows.

In each case, although the Sacramento River has the largest flow among the individual rivers and also the largest flow variability, the flow from the middle-altitude basins of the central Sierra rivers (Feather, Yuba, and American) with their large runoff rates and greater sensitivity to precipitation timing and temperature fluctuations plays the leading role in determining salinity variations. During the critical winter and spring 'management' season (focused on February–June), salinity responses shift from an early domination by central Sierra and Sacramento River variations to a domination by central and southern Sierra variations late in the season. Prediction or management, depending on season, of salinities throughout much of the year are likely to be necessary to balance the competing interests of water deliveries for municipal and agricultural users across the State, for fisheries preservation, and for the local health of the Bay and its surroundings. Our results indicate that prediction and management of salinities in San Francisco Bay, especially in the crucial February to June period, will depend on planning and, ultimately, prediction of interseasonal streamflow variations all along the western slope of the Sierra Nevada, but perhaps especially in the central middle-altitude river basins.

Acknowledgements

Gary Hester, California Department of Water Resources, provided the full-natural flow estimates and helpful discussions. Larry Riddle of Scripps Institute of Oceanography and Richard Smith, US Geological Survey, provided several of the hydroclimatic and salinity series, respectively. Thoughtful comments from Noah Knowles, Scripps Institution of Oceanography; Mark Stacey, Stanford University; and several anonymous reviewers helped to focus this paper. This analysis is a product of the US Geological Survey's San Francisco Bay Place-Based Science Program.

References

Aguado, E., Cayan, D.R., Riddle, L.G., Roos, M., 1993. Climatic fluctuations and the timing of West Coast streamflow. J. Clim. 5, 1468–1483.

California Department of Water Resources, 2000. Management of the California State Water Project. Bulletin 132-00, 369 pp.

Cayan, D.R., Peterson, D.H., 1989. The influence of North Pacific atmospheric circulation on streamflow in the west. AGU Geophysical Monograph 55, 375–396.

Cayan, D.R., Peterson, D.H., 1993. Spring climate and salinity in the San Francisco Bay estuary. Water Resour. Res. 29, 293–303.

Cayan, D.R., Webb, R.H., 1993. El Niño/Southern Oscillation and streamflow in the United States. In: Diaz, H.F., Markgraf, V. (Eds.), El Niño: Historical and Paleoclimatic Aspects of the Southern Oscillation, Cambridge University Press, Cambridge, pp. 29–68.

Cayan, D.R., Riddle, L.G., Aguado, E., 1993. The influence of precipitation and temperature on seasonal streamflow in California. Water Resour. Res. 29, 1127–1140.

Cayan, D.R., Kammerdiener, S., Dettinger, M.D., Caprio, J.M., Peterson, D.H., 2001. Changes in the onset of spring in the western United States. Bull. Am. Meteorol. Soc. 82, 399–415.

Dettinger, M.D., Cayan, D.R., 1992. Climate-change scenarios for the Sierra Nevada, California, based on winter atmospheric-circulation patterns. Proceedings of the 1992 AWARA Annual Symposium and Conference, Managing Water Resources under Global Change, Reno. Nev., pp. 681–690.

Dettinger, M.D., Cayan, D.R., 1995. Large-scale atmospheric forcing of recent trends toward early snowmelt in California. J. Clim. 8, 606–623.

Dettinger, M.D., Cayan, D.R., Diaz, H.F., Meko, D.M., 1998. North–south precipitation patterns on interannual–decadal timescales. J. Clim. 11, 3095–3111.

Guttmann, L., 1954. Some necessary conditions for common-factor analysis. Psychometrika 19, 146–161.

Jassby, A.D., Kimmerer, W.J., Monismith, S.G., Armor, C., Cloern, J.E., Powell, T.M., Schubel, J.R., Vendlinski, T.J., 1995. Isohaline position as a habitat indicator for estuarine populations. Ecol. Appl. 5, 272–289.

Jassby, A.D., Koseff, J.R., Monismith, S.G., 1996. Processes underlying phytoplankton variability in San Francisco Bay. In: Hollibaugh, J.T., (Ed.), San Francisco Bay—The Ecosystem, Pacific Division, AAAS, San Francisco, CA, pp. 325–349.

Jeton, A.E., Dettinger, M.D., Smith, J.L., 1996. Potential effects of climate change on streamflow, eastern and western slopes of the Sierra Nevada, California and Nevada. US Geological Survey Water Resources Investigations Report 95-4260, 44 pp.

Kennish, M.J., 2000. Estuary Restoration and Maintenance—The National Estuary Program, CRC Press, Washington, DC, 359 p.

Kimmerer, W.J., Orsi, J.J., 1996. Changes in the zooplankton of the San Francisco Bay estuary since the introduction of the clam Patamocorbula amurensis. In: Hollibaugh, J.T., (Ed.), San Francisco Bay—The Ecosystem, Pacific Division, AAAS, San Francisco, CA, pp. 403–424.

Knowles, N., 2000. Modeling the hydroclimate of the San Francisco Bay—Delta Estuary and Watershed. PhD Dissertation, Scripps Institution of Oceanography, 291 pp.

Knowles, N., 2002. Natural and management influences on freshwater inflows and salinity in the San Francisco Estuary at monthly to interannual scales. Water Resour. Res. 38, 25–1 to 25–11.

Leather, D.J., Yarnal, B., Palecki, M.A., 1991. The Pacific/North American teleconnection pattern and United States climate. Part I. Regional temperature and precipitation associations. J. Clim. 4, 517–528.

Legates, D.R., 1991. The effect of domain shape on principal components analyses. Int. J. Climatol. 11, 135–146.

Legates, D.R., 1993. The effect of domain shape on principal components analyses: a reply. Int. J. Climatol. 13, 219–228.

North, G.R., Bell, T.L., Cahalan, R.F., Moeng, F.J., 1982. Sampling errors in the estimation of empirical orthogonal functions. Mon. Wea. Rev. 110, 699–706.

Peterson, D.H., 1995. Seasonal/yearly variations in San Francisco Bay. US Geological Survey Fact Sheet, 4 pp.

Peterson, D.H., Cayan, D.R., Festa, J.F., Nichols, F.H., Walters, R.A., Slack, J.R., Hager, S.W., Schemel, L.E., 1989. Climate variability in an estuary: effects of riverflow on San Francisco Bay. In: Peterson, D.H., (Ed.), Geophysical Monograph 55, Aspects of Climate Variability in the Pacific and the Western Americas, AGU, Washington, DC, pp. 419–442.

Peterson, D.H., Cayan, D.R., DiLeo, J., Noble, M., Dettinger, M.D., 1995. The role of climate in estuarine variability. Am. Sci. 83, 58–67.

Peterson, D.H., Cayan, D.R., Dettinger, M.D., Noble, M.A., Riddle, L.G., Schemel, L.E., Smith, R.E., Uncles, R.J., Walters, R.A., 1996. San Francisco Bay salinity: observations, numerical simulations, and statistical models. In: Hollibaugh, J.T., (Ed.), San Francisco Bay: The Ecosystem, Pacific Division, AAAS, San Francisco, CA, pp. 9–34.

Philander, S.G., 1990. El Niño, La Niña, and the Southern Oscillation, Academic Press, San Diego, CA, 289 p.

Press, W.H., Flannery, B.P., Teukolsky, S.A., Vettering, W.T., 1989. Numerical Recipes—The Art of Scientific Computing (FORTRAN Version), Cambridge University Press, New York, 702 pp.

Richman, M.B., 1986. Rotation of principal components. Int. J. Climatol. 6, 293–335.

Richman, M.B., 1993. Comments on: the effect of domain shape on principal components analyses. Int. J. Climatol. 13, 203–218.

Stahle, D., Therrell, M., Cleaveland, M.K., Cayan, D.R., Dettinger, M.D., Knowles, N., 2001. Ancient Blue oaks reveal human impact on San Francisco Bay salinity. EOS, Trans. Am. Geophys. Union 82, 144–145.

State of California, 1986. Day flow program documentation and day flow data summary user's guide. California Department of Water Resources, Central District, (3521) S Street, Sacramento, CA.

von Storch, H., 1995. Spatial patterns—EOFs and CCA. In: Storch, H., Navarra, A. (Eds.), Analysis of Climate Variability—Applications of Statistical Techniques, Springer, New York, pp. 227–257.

Weare, B.C., Nasstrom, J.S., 1982. Examples of extended empirical orthogonal function analysis. Mon. Wea. Rev. 110, 481–485.